



AIAA 94-2896

**A Neutronic Study of the Open-Cycle
Gas Core Nuclear Rocket**

D.I. Poston and T. Kammash

The University of Michigan

Ann Arbor, MI

**30th AIAA/ASME/SAE/ASEE Joint
Propulsion Conference**

June 27-29, 1994 / Indianapolis, IN

A NEUTRONIC STUDY OF THE OPEN-CYCLE GAS CORE NUCLEAR ROCKET

David I. Poston and Terry Kammash
 Department of Nuclear Engineering
 University of Michigan
 Ann Arbor, MI

Abstract

The neutronic characteristics of the open-cycle Gas Core Nuclear Rocket (GCR) are studied. In the first portion of the paper, a parametric analysis is performed which investigates how k_{eff} varies as a function of several design parameters. The parameters varied include the temperature and composition of the fuel and propellant, as well as the moderator thickness. In the second portion of the paper, the neutronic model is coupled with a thermal-hydraulic model that solves the 2-D steady state conservation equations of mass, species, axial momentum, radial momentum, and energy. The neutronic solution of one particular design is studied in detail, including the spatial variation of power density, neutron flux, and neutron energy spectra. Finally, the effect of using alternate fuels and propellants is examined.

Introduction

In the Gas Core Nuclear Rocket (GCR), a fissioning plasma heats a low-Z propellant (primarily by radiation), which is exhausted through a choked nozzle. In the open-cycle GCR there is no physical barrier between the fuel and propellant; therefore, the flow field must be constructed in a manner which minimizes fuel/propellant mixing. The open-cycle GCR has the potential to deliver astounding rocket performance. Poston and Kammash^[1] found that if the fuel and propellant can be prevented from mixing, a 3000 MW reactor can produce a specific impulse of 3160 s with a thrust of 125 kN (assuming a maximum wall heat flux of 100 MW/m²). However, when fuel/propellant mixing was added to this model^[2], the specific impulse dropped by approximately a factor of two. The limit on rocket performance was not imposed by heat transfer or fluid flow issues, but by neutronic considerations. To obtain a critical design, the power had to be lowered or the fuel mass flow rate had to be increased, thus causing a drop in specific impulse.

This study was initiated in order to better understand the neutronic characteristics of the open-cycle GCR, and consequently, how to better achieve criticality. In the first portion of the paper, a parametric analysis is performed which investigates how k_{eff} varies as a function of the fuel/propellant composition and temperature, as well as moderator thickness. Each region of the reactor, including the fuel and propellant, is assumed to be homogenous, which makes it easier to isolate the dependence of k_{eff} on each parameter. In the second portion of the paper, the neutronic model is coupled with a Thermal-Hydraulic (T-H) model. The T-H model solves the 2-D steady state conservation equations of mass, species, axial momentum, radial momentum, and energy. To obtain a complete solution, the thermal-hydraulic and neutronic solutions are iterated until a consistent power density is obtained. The neutronic solution of one particular design is studied in detail, including the spatial variation of fission rate, neutron flux, and neutron energy spectra. In the final portion of the paper, the effect of using alternate fuels and propellants is examined.

Analysis

A complete thermal-hydraulic/neutronic model of an open-cycle GCR has been developed. This paper examines only the neutronic aspects of the system; the thermal-hydraulics have been discussed in previous papers by Poston and Kammash. Some requirements of the neutronic model are:

- Upscattering
- Many Energy Groups
- Highly Inhomogenous Mesh
- Output Tailoring

The code chosen for this analysis is the transport neutronics code TWODANT. Fifty group cross sections were obtained from EG&G Idaho for a wide range of materials and temperatures^[3], including isotropic and linearly anisotropic differential scattering matrices. For all cases presented in this paper, first order anisotropic scattering is included, and a quadrature order of $S_N=4$ is used. The

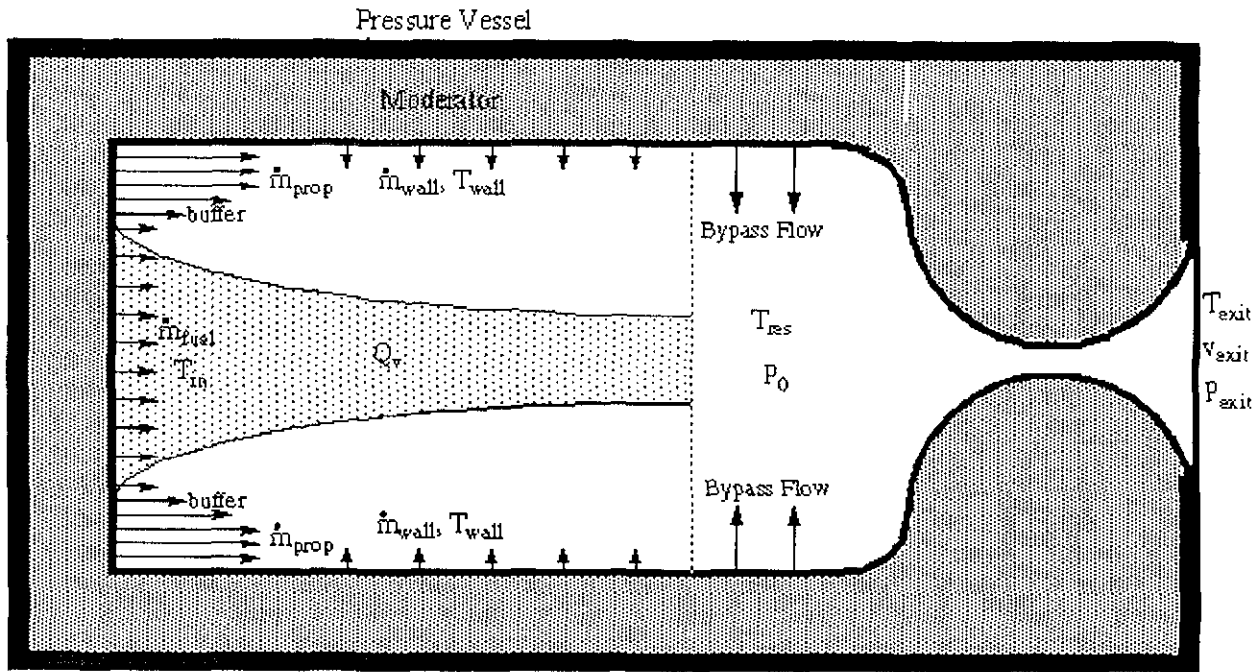


Fig. 1. Schematic of the open-cycle gas core nuclear rocket computational model.

materials considered in this analysis are listed in Table 1.

Table 1. Materials considered.

Region	Materials
Fuel	U-235,U-233,Pu-239
Propellant	H,D,He
Moderator	BeO
Vessel	Ti

The neutronic analysis of the open-cycle GCR is performed in two stages. The first phase of the research qualitatively studies the neutronic behavior of a homogeneous cylindrical open-cycle GCR. A parametric analysis is performed which examines how k_{eff} varies with the density and temperature of the fuel and propellant. A reactor with homogenous fuel and propellant regions is used so that the effects of varying density and temperature can more easily be isolated.

The second portion of this paper involves the linking of the thermal-hydraulic and neutronic models. The thermal-hydraulic model that is used to perform this analysis obtains a numerical solution of the Navier-Stokes, energy, and species diffusion

equations as a function of design and operational parameters. A schematic of the model is shown in Figure 1. The fuel and propellant enter the reactor with a constant mass flow rate; the propellant surrounds the fuel in the shape of a cylindrical annulus. The propellant enters the reactor with a user-specified velocity profile, which includes: the inlet and wall mass flow rates, the buffer zone dimensions, and the injection velocity and angle of wall flow. If the maximum wall heat flux is reached, the propellant flow through the wall is increased to provide transpiration cooling. In addition to the flow rates; the system dimensions, material limitations, power, and boundary conditions are used as code input. The T-H model is described in detail in Poston and Kammash^[4].

The T-H and neutronic models are linked in the following manner. First, a T-H solution is produced assuming a constant and uniform neutron flux, thus the power density is directly dependent on fuel density. The T-H model produces a TWODANT input file based on the fuel/propellant densities and temperatures at each node. Next TWODANT is run, and upon completion TWODANT generates an edit file containing the neutron flux times the microscopic fission cross section. This file is used in return by the T-H model to calculate the power

density. This iteration continues until the power density and flux converge to their respective asymptotic values.

Results and Discussion

Homogeneous Reactor

To begin, a parametric analysis is performed on a cylindrical homogeneous reactor design. The composition and dimensions (L=fuel axial dimension, R=fuel radius) of the anchor point for the parametric analysis are listed in Table 2.

Table 2. Homogeneous Design.

Region	Material	Thick. (cm)	Temp. (K)
Fuel	U-235	L=200,R=100	50,000
Propellant	H	20	10,000
Moderator	BeO	30	1,200
Vessel	Ti	10	not spec.

The composition of the pressure vessel has no significant impact on the solution except for mass (provided that the moderator is thick enough to dominate the neutronics), thus titanium was selected for its high strength to weight ratio. In reality, many other factors will be used in determining the ideal pressure vessel material.

The first parameter varied is the fuel density. The multiplication factor k-eff is plotted versus fuel density in Figure 2. The fuel density is normalized to (divided by) the density at 50,000 K and 1000 atm. K-eff increases significantly as the density increases up to about a factor of five. This shows the

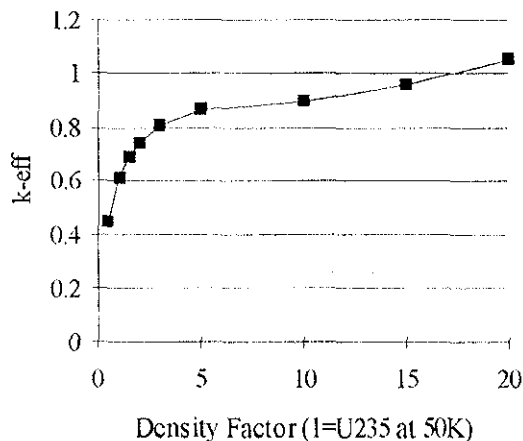


Fig. 2. Fuel Density Varied.

importance of operating the reactor at as high of pressure as possible. Unfortunately, it is not very likely that pressures much greater than 1000 atm could be achieved in the near future. The increase in k-eff levels off between density factors of 5 and 15, and then begins to rise again. This second rise occurs because at densities this high, the open-cycle GCR begins to resemble a bomb more than a propulsion device.

To study the effect of propellant temperature and density on k-eff, three cases were tested. First, the density of the propellant was varied while holding the temperature constant (in effect varying the pressure in the propellant region only). The effect of changing the density of 10,000 K hydrogen is plotted in Figure 3. As the density factor increases from 0 to 2, there is a sharp drop in k-eff. This is because the hydrogen is serving as a poison to the nuclear reaction. The hydrogen is not dense enough to moderate the neutrons, however it is dense enough to hinder the migration of thermalized neutrons from the moderator to the fuel. To make matters worse, many of the hydrogen atoms are at higher energies than the thermalized neutrons, so there is considerable upscattering. Notice that as the propellant density increases above a factor of 5, k-eff begins to increase. At this point the hydrogen is dense enough to somewhat moderate (at least to epithermal energies) and reflect the neutrons, and the reactor is shifting from a thermal to a epithermal/fast reactor.

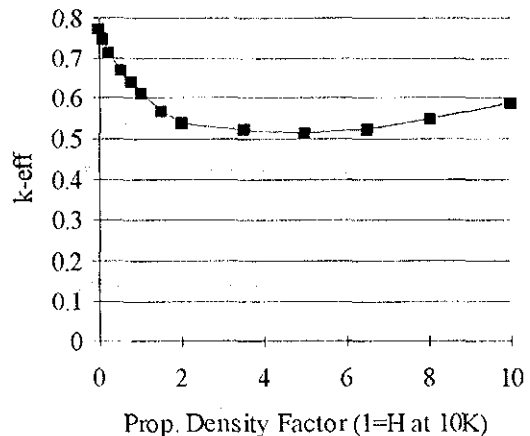


Fig. 3. Propellant Density Varied (const. temp.).

In Figure 4 the temperature of the propellant is varied while holding the density constant (once again effectively changing the pressure). The

purpose of this plot is to demonstrate the effect that upscattering has on the solution. As expected, k_{eff} drops sharply as the temperature of the hydrogen is increased.

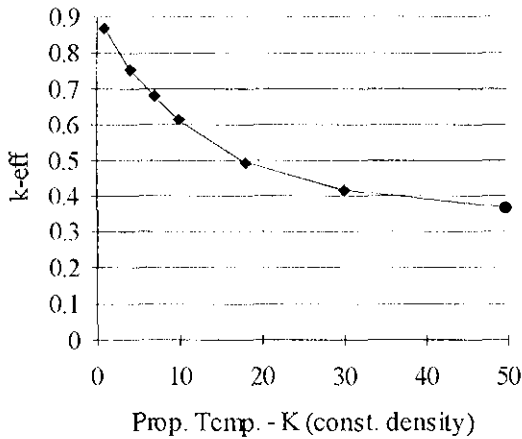


Fig. 4. Propellant Temp. Varied (const. density).

Figure 5 plots k_{eff} versus propellant temperature (at constant pressure=1000 atm), thus combining the effects seen in Figures 3 and 4. At temperatures less than 3,000 K, increasing the temperature boosts k_{eff} because the benefit of decreased density outweighs the detrimental effect of increased upscattering. Between 3,000 K and 20,000 K the upscattering dominates, causing k_{eff} to drop, but beyond 20,000 K k_{eff} begins to rise again. Unfortunately, most of the hydrogen in a high performance GCR has a temperature between 10,000 K and 20,000 K, which is the area of lowest

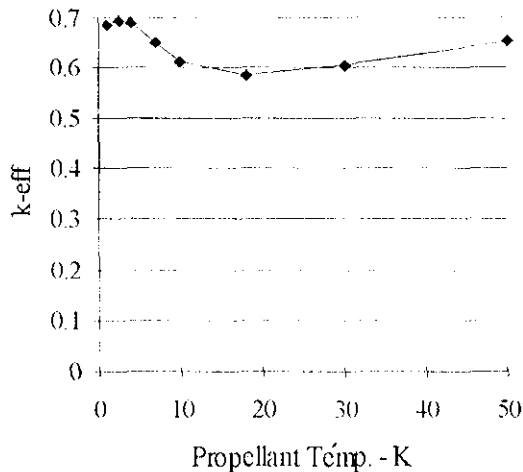


Fig. 5. Propellant Temperature Varied.

k_{eff} on the chart.

Finally, the homogenous reactor design was used to evaluate moderator worth. K_{eff} is plotted versus moderator thickness in Figure 6. The moderator worth is very high up to a thickness of 40 cm. Increasing the moderator thickness to more than 40 cm has little effect because any neutron that requires such a large of distance to moderate will most likely not make it back to the core. It also must be noted that any increase in moderator thickness has a very large impact of reactor mass, especially since the moderator begins at a radius of 1.5 m. Therefore, for the base case a moderator thickness of 30 cm has been chosen.

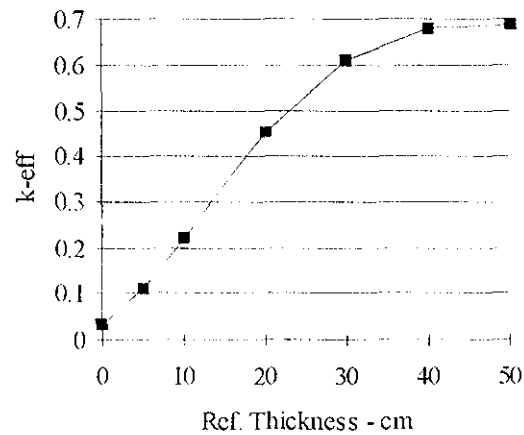


Fig. 6. Moderator Thickness Varied.

Coupled T-H/Neutronic Solution

The input parameters of the design chosen for the coupled thermal-hydraulic/neutronic analysis are listed in Table 3.

Table 3. T-H/Neutronic Input Parameters.

Reactor Power (MW)	500
Reactor Pressure (atm)	1000
Propellant Flow Rate (kg/s)	3.0
Fuel Flow Rate (kg/s)	1.0
Inlet & Wall Temp. (K)	2200
Core Length	2.00
Fuel Radius at Inlet (m)	1.20
Buffer Zone Outer Rad. (m)	1.35
Outer Wall Radius (m)	1.50
Moderator Thickness (cm)	30
Fuel Material	U-233
Propellant Material	H

The iteration between the T-H and neutronic models proceeded as described in the Analysis section. The solution converged in less than ten iterations without relaxation (less iterations would be required if under-relaxation was utilized). The key results of the combined T-H/neutronic model are listed in Table 4.

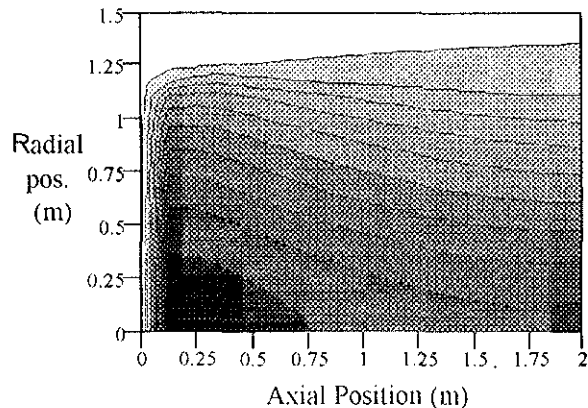
Table 4. T-H/Neutronic Results.

Fuel Outlet Temp. (K)	34,800
Prop. Outlet Temp. (K)	5,920
Specific Impulse (s)	1380
Thrust (kN)	54.2
Avc. Fuel Density (#/m ³)	6.31E+24
Fuel Loading (kg)	37.4
Prop. Loading (kg)	48.0
Multiplication Factor, k-eff	.852

Figures 7 through 11 display two-dimensional contour plots for temperature, mole fraction, fuel number density, neutron flux times fission cross section, and power density. On these plots, the radial position R=0 corresponds to the centerline, while R=1.5 is the outer wall. The axial position Z=0 represents the core inlet, and Z=2 is the end of the core region.

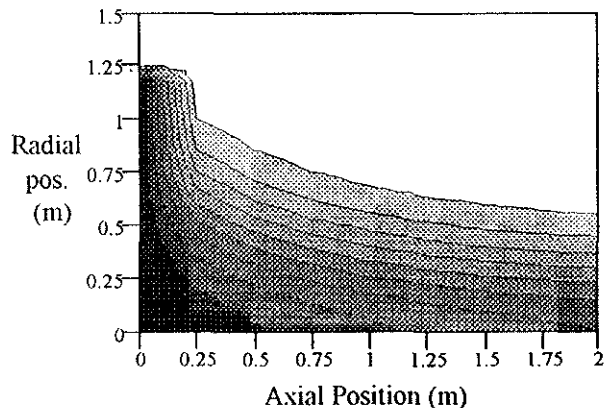
The temperature is plotted in Figure 7. There is a localized region of hot fuel near the inlet, and then temperatures in the fuel region begin to drop downstream due to an influx of hydrogen. The hydrogen lowers the overall temperature because of its lower temperature and its relatively high specific heat. Figure 8 contains a contour plot of fuel mole fraction. The mole fraction drops rapidly as the flow

moves downstream, due to both convective and diffusive mixing. Unfortunately, the convective mixing becomes much more pronounced as the power level increases. The most important result of the T-H model is the fuel number density, which is plotted in Figure 9. The fuel density does not drop as quickly as mole fraction due to the drop in temperatures as the flow move downstream. In fact, the highest density region turns out to be closer to the exit than the inlet. Figure 10 plots the neutron flux times the microscopic fission cross section - or the fission inducing flux. This could also be thought of as a plot of thermal neutron flux (although in U-233 many fissions occur in the epithermal range as well), with the darkest regions representing the highest thermal neutron flux. Figure 10 shows that only a small number of the thermal neutrons are reaching the fuel. The fission inducing flux is high at the boundaries (near the moderator) and drops rapidly as the neutrons encounter the propellant. Careful examination of Figure 10 reveals the effect of propellant temperature on upscattering. At the upper left corner of the plot, where hydrogen temperatures are low, the thermal neutrons penetrate further into the core than in the upper right corner, where temperatures are higher. The other barrier to thermal neutron penetration is the fuel itself, which explains why the fission inducing flux is higher in the lower right quadrant than the lower left quadrant. Figure 11 plots the power density, which is proportional to the fuel number density times the fission inducing flux. Hot spots appear along the axial boundaries due to the proximity of the moderator.



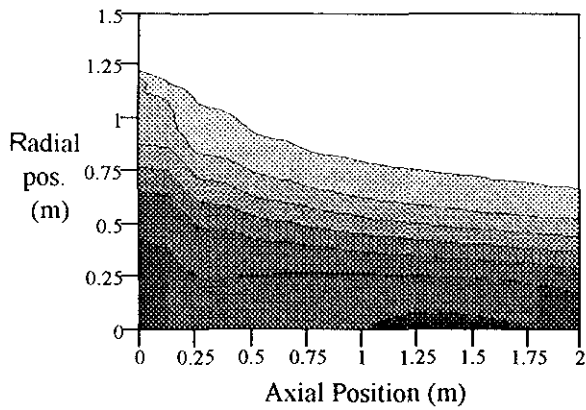
Each contour line represents 5,000K ranging from 5,000K (light) to 50,000K (dark).

Fig. 7. Temperature Contour Plot.



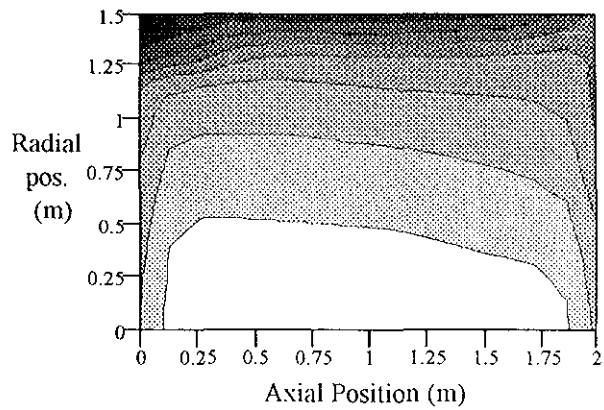
Each contour line represents .1 ranging from .1 (light) to .9 (dark).

Fig. 8. Fuel Mole Fraction Contour Plot



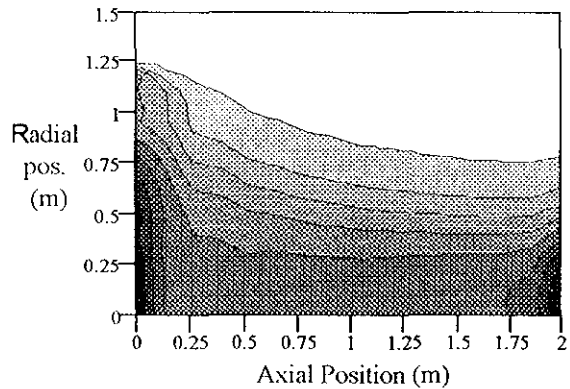
Each contour line represents $5E^{24} \text{ m}^{-3}$ ranging from $5E^{24} \text{ m}^{-3}$ (light) to $3.5E^{25} \text{ m}^{-3}$ (dark).

Fig. 9. Fuel Number Density Contour Plot.



Each contour line represents $.05\mu\text{s}$ ranging from $.15\mu\text{s}$ (light) to $.45\mu\text{s}$ (dark).

Fig. 10. Flux times σ_{fis} Contour Plot



Each contour line represents 25MW/m^3 ranging from 25MW/m^3 (light) to 200MW/m^3 (dark).

Fig. 11. Power Density Contour Plot.

To get a more detailed look at the flux distribution, the radial flux profile at the axial center of the core is displayed in Figure 12. At the midplane the fuel/propellant interface is at about .7 m, and the moderator begins at 1.5 m. As expected, the fast neutron flux is highest in the fuel region, where the fissions take place. The thermal flux is highest along the inner edge of the moderator and drops off quickly in both directions. Figure 12 verifies that the thermal neutrons are not reaching the fuel. The slight increase in epithermal flux moving from 1.5 m to 1.0 m is due mainly to upscattering.

The final task is to evaluate the above design for different combinations of fuels and propellants. The results for each combination tested are in Table 5. In Table 5, only the nuclear properties of each material are changed from case to case. In each case the fuel is assumed to have the thermodynamic properties of U-235, and the propellant is assumed to have the thermodynamic properties of hydrogen. This assumption is reasonable for the fuel, but not for the propellant. The effect of the assumption will be discussed later.

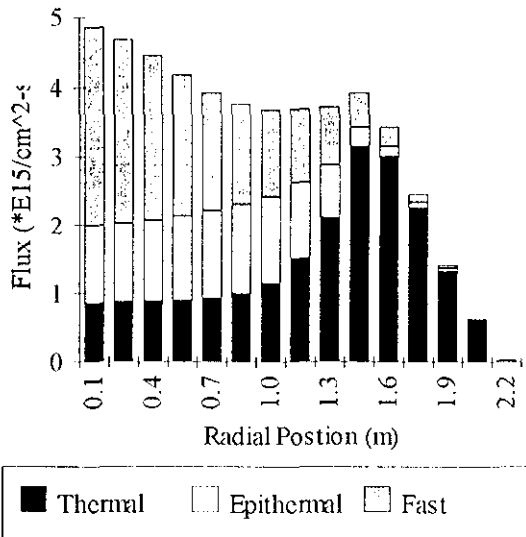


Fig. 12. Radial Flux Profile at Core Midplane.

Table 5. k-eff for Various Combinations

Fuel	Prop.	k-eff
U-235	H	.534
U-233	H	.852
Pu-239	H	.754
U-235	He	.879
U-233	He	1.001
Pu-239	He	.938

The advantage of using U-233 in a GCR is demonstrated by looking at the fission cross sections of each fuel. Figure 13 shows the microscopic fission cross section of U-235, U-233, and Pu-239 at thermal and epithermal energies. U-235 has its highest cross sections at the lowest energies. Pu-239 has some very large cross sections between .3ev and .5ev, but also has no significant cross sections above 1ev. U-233 is similar to U-235 at thermal energies, however the fission cross section becomes quite large between 1ev and 2ev. These energies are very significant because of the temperature of the propellant. If the propellant is hydrogen, which has essentially the same mass as a neutron, then hydrogen/neutron collisions will tend to bring the neutrons and hydrogen atoms to the same energy. Considering that 11,500K corresponds to an energy of 1ev, and that much of the hydrogen is at a

temperature greater than 10,000K, then many of the thermal neutrons will upscatter to energies greater than 1ev. This explains why U-233 is the best fuel choice for this design (of course ignoring many other factors including cost).

Using helium as the propellant instead of hydrogen causes a significant improvement in k-eff. At equal temperatures, helium moves at half the speed of atomic hydrogen; therefore, there is much less upscattering. Not surprisingly, the improvement when changing from hydrogen to helium is most dramatic in U-235, which depends most on thermal neutrons to produce fissions. Unfortunately, the property of helium (heavier mass) that makes it better than hydrogen neutronically, has a detrimental effect on rocket performance. The specific impulse is inversely proportional to the square root of the mass; thus, the specific impulse will drop approximately by a factor of two when changing from hydrogen to helium. Consequently, in most cases the best choice of propellant will be hydrogen. The only way to exactly predict which propellant is superior would be to solve the T-H model using the thermodynamic properties of helium, instead of assuming that the propellant has the thermodynamic properties of hydrogen and the nuclear properties of helium.

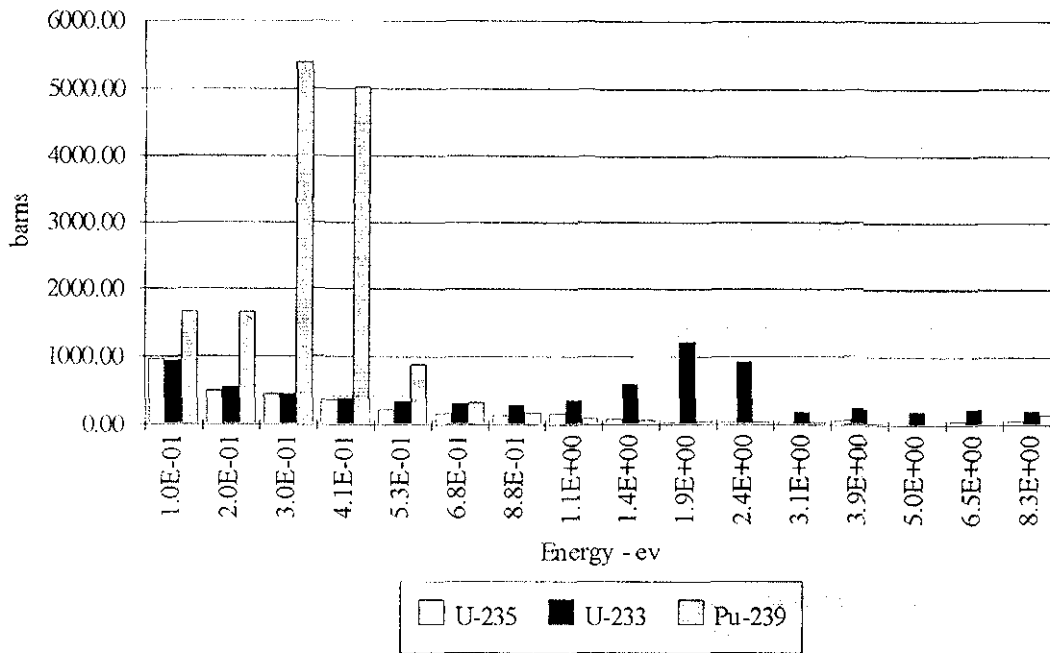


Fig. 13. Microscopic Fission Cross Sections at Low Energies

Conclusions

The neutronic characteristics of the open-cycle gas core nuclear rocket are studied. The qualitative effects of fuel/propellant temperature and density on neutronics are studied by analyzing a homogenous reactor. Particular attention is applied to the effects of neutron upscattering (due to the high temperature propellant) on achieving criticality. The multiplication factor is found to be lowest for hydrogen temperatures between 10,000 K and 20,000 K. A coupled thermal-hydraulic/neutronic solution is studied, and several different materials are considered for use as the fuel and the propellant. From a neutronic standpoint, the best fuel and propellant combination of those studied is U-233 and helium. However, U-233 and hydrogen yield the best overall rocket performance.

Acknowledgments

This work was supported by the NASA Lewis Research Center as part of the NASA Graduate Student Researchers Program. The authors would like to acknowledge John Clark and Stan Borowski at NASA Lewis and Bruce Schnitzler at EG&G Idaho for their assistance.

References

1. D.I. Poston and T. Kammash (1992) "Heat Transfer Model for an Open-Cycle Gas Core Nuclear Rocket". *Proc. 9th Symposium on Space Nuclear Power Systems*, American Institute of Physics, AIP Conf. Proc. No. 246, 3:1083-1088.
2. D.I. Poston and T. Kammash (1994) "Hydrodynamic Fuel Containment in an Open-Cycle Gas Core Nuclear Rocket". *Proc. 11th Symposium on Space Nuclear Power and Propulsion*, American Institute of Physics, AIP Conf. Proc. No. 301, 1:473-479.
3. B.G. Schnitzler (1990) "Gas Core Reactors for Direct Nuclear Propulsion". Idaho National Engineering Lab., Report # EGG-NE-9087.
4. D.I. Poston and T. Kammash (1994) "A Comprehensive Thermal-Hydraulic Model of an Open-Cycle Gas Core Nuclear Rocket". *Proc. 11th Symposium on Space Nuclear Power and Propulsion*, American Institute of Physics, AIP Conf. Proc. No. 301, 3:1415-1520.